Malondialdehyde induces autophagy dysfunction and VEGF secretion in the retinal pigment epithelium in age-related macular degeneration

Fuxiang Ye[1 §], Hiroki Kaneko[1 §*], Yumi Hayashi[2,3], Kei Takayama[1], Shiang-Jyi Hwang[1,4], Yuji Nishizawa[5], Reona Kimoto[1], Yosuke Nagasaka[1], Taichi Tsunekawa[1], Toshiyuki Matsuura[1], Tsutomu Yasukawa[6], Takaaki Kondo[2], and Hiroko Terasaki[1]

[1]Department of Ophthalmology, Nagoya University Graduate School of Medicine, Nagoya 466-8550, Japan

[2]Department of Radiological and Medical Laboratory Sciences, Nagoya University Graduate School of Medicine, Nagoya 461-8673, Japan

[3]Institute for Advanced Research, Nagoya University, Nagoya 464-8601, Japan

[4]Laboratory of Bell Research Center–Department of Obstetrics and Gynecology collaborative research, Nagoya University Graduate School of Medicine, Nagoya 466-8550, Japan

[5]Department of Biomedical Sciences, Chubu University, Kasugai, Aichi 487-8501, Japan

[6]Department of Ophthalmology, Nagoya City University School of Medicine, Nagoya 467-8601, Japan

[§]These authors contributed equally to this work.

*Author for correspondence: Hiroki Kaneko, Department of Ophthalmology, Nagoya University Graduate School of Medicine, 65 Tsurumai-cho, Showa-ku, Nagoya 466-8550, Japan. E-mail address: h-kaneko@med.nagoya-u.ac.jp

Highlights

- Malondialdehyde accumulated in the sera and eyes of patients with AMD.
- VEGF secretion in RPE cells was dysregulated by malondialdehyde.
- Malondialdehyde induced RPE cell junction disruption and autophagy dysfunction.
- Administration of malondialdehyde increased CNV volumes in mice.
- Higher dietary intake of linoleic acid promoted CNV progression in mice.

Graphical abstract

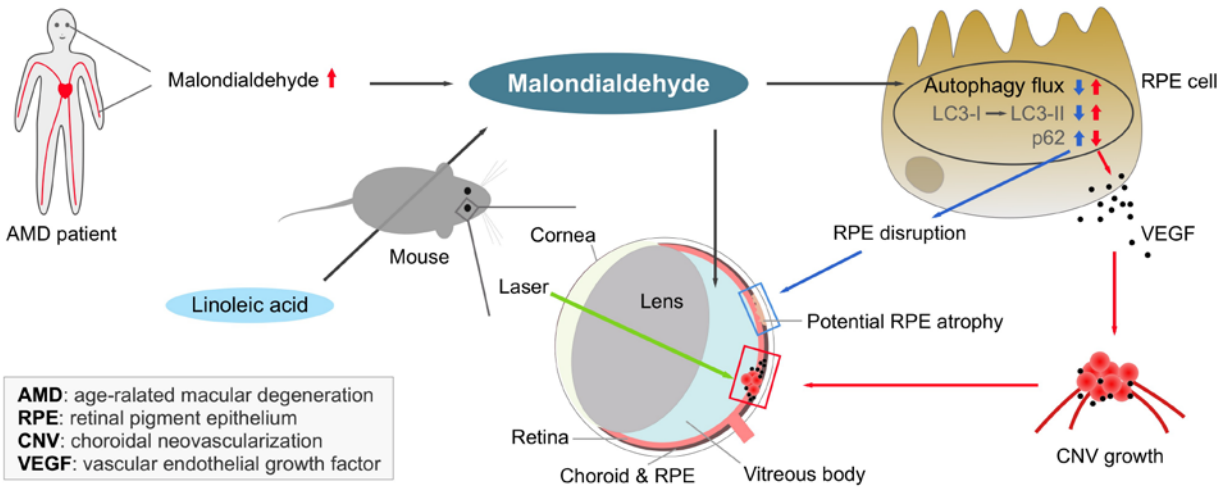

Abstract

Age-related macular degeneration (AMD) is a major cause of blindness in developed countries and is closely related to oxidative stress, which leads to lipid peroxidation. Malondialdehyde (MDA) is a major byproduct of polyunsaturated fatty acid (PUFA) peroxidation. Increased levels of MDA have been reported in eyes of AMD patients. However, little is known about the direct relationship between MDA and AMD. Here we show the biological importance of MDA in AMD pathogenesis. We first confirmed that MDA levels were significantly increased in eyes of AMD patients. In ARPE-19 cells, a human retinal pigment epithelial cell line, MDA treatment induced vascular endothelial growth factor (VEGF) expression alternation, cell junction disruption, and autophagy dysfunction that was also observed in eyes of AMD patients. The MDA-induced VEGF increase was inhibited by autophagy–lysosomal inhibitors. Intravitreal MDA injection in mice increased laser-induced choroidal neovascularization (laser-CNV) volumes. In a

mouse model fed a high-linoleic acid diet for 3 months, we found a significant increase in MDA levels, autophagic activity, and laser-CNV volumes. Our study revealed an important role of MDA, which acts not only as a marker but also as a causative factor of AMD pathogenesis-related autophagy dysfunction. Furthermore, higher dietary intake of linoleic acid promoted CNV progression in mice with increased MDA levels.

Key words: Age-related macular degeneration; Lipid peroxidation; Malondialdehyde; Autophagy; Linoleic acid

List of abbreviations

AMD = age-related macular degeneration, MDA = malondialdehyde, LA = linoleic acid, HLA = high linoleic acid, AA = arachidonic acid, RPE = retinal pigment epithelium, VEGF = vascular endothelial growth factor, POS = photoreceptor outer segments, TER = transepithelial resistance, ZO-1 = zonula occludens-1, CNV = choroidal neovascularization, PUFA = polyunsaturated fatty acid, NH_4Cl = ammonium chloride, 3-MA = 3-methyladenine, RIPA = radioimmunoprecipitation assay, PFA = paraformaldehyde, SIM = selected ion monitoring

Introduction

Age-related macular degeneration (AMD) is a leading cause of blindness in developed nations [1, 2]. Based on the manifestation, AMD is differentiated into two types: wet and dry AMD. Wet AMD is characterized by the presence of choroidal neovascularization (CNV), which is strongly related to overexpression of the proangiogenic cytokine vascular endothelial growth factor (VEGF). Dry AMD is characterized by geographic atrophy of the retinal pigment epithelium (RPE) [3, 4]. Anti-VEGF antibody treatment is the current standard treatment for wet AMD [5-7]; however, some wet AMD eyes show recurrence, with persistent CNV in response to repeated anti-VEGF injections [8, 9]. Furthermore, even after repeated injections of anti-VEGF antibodies, some eyes retain severe RPE atrophy [10]. Therefore, improved understanding of the mechanisms underlying RPE conditions and promotion of VEGF upregulation in AMD eyes is necessary. Known risk factors of AMD are obesity, hypertension, and smoking [11-13]. In addition, recent studies have shown that oxidative stress is strongly related to AMD pathogenesis [1, 14].

Malondialdehyde (MDA) is a highly reactive three-carbon dialdehyde produced as a byproduct of polyunsaturated fatty acid (PUFA) peroxidation, which is catalyzed by free radicals [15, 16]. High levels of PUFAs are found in vegetable oils, which are usually considered beneficial for health. In fact, it is generally recommended that animal fats, which are rich in saturated fatty acids, be replaced by vegetable oils in the diet [17]. However, recent studies have suggested that high intake of dietary linoleic acid (LA), an ω-6 fatty acid and the most abundant dietary PUFA, is a risk factor for several cancers [18] and heart diseases [19]. Photoreceptor outer segments (POS) are rich in unsaturated fatty acids, and MDA is generated as a result of oxidation of these unsaturated fatty acids. Consistently, MDA is found in the drusen, which are extracellular deposits that accumulate in AMD eyes [20, 21]. Although MDA is used as a biological marker of oxidative stress [22], it has also been reported to be toxic, mutagenic, and carcinogenic [23]. In fact, some studies have shown that MDA induces cytotoxicity and VEGF expression in RPE cells *in vitro* [24-26]. In addition, recent studies have suggested that MDA levels are higher in the blood of AMD patients than in that of healthy subjects [27-29]. However, little is known regarding the factors that trigger MDA-induced changes in the pathogenesis of AMD, which is thought to be a localized eye disease, particularly in the most secluded areas of the eye. Moreover, it is difficult to make direct

correlations between general changes in eyes and AMD progression.

Therefore, the present study aimed to determine whether MDA levels are elevated in the serum and RPE of patients with AMD and to assess the biological importance of MDA in the pathogenesis of AMD in animal and cellular models.

Materials and methods

Human eyes and sera

Donor eyes from control subjects and patients with AMD were obtained from the Minnesota Lions Eye Bank (St. Paul, MN, USA) and used for MDA quantification and western blot analysis. Another three donor eyes were obtained from the San Diego Eye Bank (San Diego, CA, USA) for immunohistochemical analysis: the first one from a patient with wet AMD, second one from a patient with dry AMD, and third one from a control subject. The diagnoses were confirmed on the basis of the medical records from the ophthalmologist as well as from postmortem examination results of the eye globes under a dissecting microscope. The study followed the guidelines of the Declaration of Helsinki. The serum samples were prepared from 41 patients with wet AMD, 19 patients with dry AMD, and 34 controls. Patients with polypoidal choroidal vasculopathy, retinal angiomatous proliferation, maculopathy with myopic CNV, or CNV based on angioid streaks were excluded. The diagnosis of wet and dry AMD was established on the basis of age (>50 years), clinical examination, fundus photography, optical coherence tomography, and fluorescein fundus angiography. Patients who had wet AMD in one eye and dry AMD in the other eye were excluded from both AMD patient groups. Control sera were obtained from patients with other ocular diseases, for example, cataract, glaucoma, retinal detachment, macular hole, and epiretinal membrane. The study was approved by the Nagoya University Hospital Ethics Review Board (#2012-0340-3), and written informed consent was obtained from each patient.

Measurement of MDA levels

To measure the MDA levels in the sera prepared from mice, a malondialdehyde assay kit (NWK-MDA01; Northwest Life Science Specialties, Vancouver, WA, USA), as reported previously [22, 30], was used following the manufacturer’s instructions. To measure MDA levels in the protein lysates or human sera, an MDA adduct enzyme-linked immunosorbent assay (ELISA) kit with higher sensitivity was used, as described

previously [31, 32]. In brief, the RPE/choroid complex from human or mouse eyes was lysed in radioimmunoprecipitation assay (RIPA) buffer (Sigma-Aldrich, St Louis, MO, USA) with a protease inhibitor cocktail (Roche Diagnostics, Mannheim, Germany). The lysate was centrifuged at 15,000 rpm for 15 min at 4°C, and the supernatant was collected. The protein concentrations were determined using a Bradford assay kit (Bio-Rad, Hercules, CA, USA) with bovine serum albumin as the standard. Sera were prepared from both human subjects. The levels of MDA were measured using an Oxiselect MDA adduct ELISA kit (STA-332; Cell Biolabs, San Diego, CA, USA) according to the manufacturer's protocol. The plates were analyzed by measuring the absorbance at 450 nm using a plate reader (Bio-Rad). Duplicate evaluations were performed for each sample.

VEGF ELISA

VEGF measurement was performed as described previously [8, 24]. In brief, protein lysates were prepared according to the same procedure as that mentioned above. Mouse VEGF levels in protein lysates were measured using a mouse VEGF ELISA kit (MMV-00; R&D Systems, Minneapolis, MN, USA). Human VEGF levels were measured using a human VEGF ELISA kit (DVE00; R&D Systems) in cell culture medium following the manufacturer's instructions. The plates were analyzed by measuring the absorbance at 450 nm with reference at 570 nm using a plate reader (Bio-Rad). Duplicate evaluations were performed for each sample.

Preparation of MDA solution

MDA was prepared as described previously [33-35]. In brief, malonaldehyde bis-(dimethyl acetal), or 1,1,3,3-tetramethoxypropane (Sigma-Aldrich), was treated with HCl (pH = 1.0) for 60 min in a water bath at 50°C. The solution was further diluted as necessary with phosphate-buffered saline (PBS) and then adjusted to pH 7.4 using NaOH solution.

Porcine POS isolation and MDA modification

Porcine eyes were obtained from a local abattoir. POS were prepared following the method described by Schraermeyer et al. [36]. MDA modification of POS was performed as described previously [26, 37]. POS were incubated overnight with different concentrations of MDA solution at 4°C on a shaker to synthesize MDA-adducted

proteins.

ARPE-19 cell culture

ARPE-19, a human RPE cell line, was purchased from the American Type Culture Collection (Rockville, MD, USA). For regular (nonpolarized) culture, the cells were grown in Dulbecco's modified Eagle's medium premixed with Ham's F-12 (1:1 ratio; Sigma-Aldrich) and supplemented with 10% (v/v) fetal bovine serum (FBS) and the antibiotics streptomycin/penicillin G (Sigma-Aldrich). Different concentrations of MDA (0.1 μM, 1 μM, 10 μM, 100 μM, and 1 mM) were used to treat the ARPE-19 cells for 48 h. To inhibit autophagy–lysosomal function, 10 mM 3-methyladenine (3-MA) or 20 mM ammonium chloride (NH_4Cl) [25] was co-administered with 1 μM MDA to ARPE-19 cells for 48 h.

Polarized cell culture

Polarized ARPE-19 cell culture was performed as described previously [38-41]. In brief, ARPE-19 cells (approximately 1.65×10^5 cells/well) were seeded onto Transwell filters (12 mm internal diameter, 0.4 μm pore size; Costar Transwell; Corning, Corning, NY, USA) precoated with Matrigel (BD Biosciences, San Jose, CA, USA). The cells were maintained for 8 weeks in a mixed medium of α-modified Eagle's minimum essential medium, N1 supplement (N-6530; 5 mL/500 mL), nonessential amino acids (M-7145; 5 mL/500 mL), L-glutamine–penicillin–streptomycin (G-1146; 5 mL/500 mL), taurine (T-0625; 125 mg/500 mL), hydrocortisone (H-0396; 10 μg/500 mL), triiodothyronine (T-5516; 0.0065 μg/500 mL) (Sigma-Aldrich), and 1% (v/v) FBS. The polarized ARPE-19 cells were then treated with MDA-modified POS for 48 h. In brief, after washing with PBS three times, POS (5 mg) treated with different concentrations of MDA were diluted with culture medium and then plated on the wells. The wells with unmodified POS and medium alone were used as controls and the outer (basal) wells were filled with culture medium. The cells were grown at 37°C in a humidified atmosphere of 5% (v/v) CO_2.

WST-1 cell proliferation assay

The proliferative activities of ARPE-19 cells were evaluated with a WST-1 colorimetric assay (Roche Diagnostics), as described previously [8]. In brief, 5×10^3 ARPE-19 cells were seeded into 96-well plates and treated with different concentrations of MDA. After

48 h, the plates were analyzed by measuring the absorbance at 450 nm using a plate reader (Bio-Rad). Duplicate evaluations were performed for each sample.

Animals

Male wild-type C57BL/6J mice were purchased from CLEA Japan, Inc. (Tokyo, Japan) and randomly assigned to standard cages containing 4–5 animals per cage and kept in standard housing conditions under a 12-h light/dark cycle. To examine MDA effects on CNV growth, mice aged 6–8 weeks that were fed a basal diet (CE-2; CLEA) were used, and 1 μL of 10 μM MDA was intravitreally injected. To generate high-MDA mice, the mice were housed with *ad libitum* access to water and CE-2-based food without fishmeal (CLEA) containing 15% (w/w) LA (Wako, Osaka, Japan) for 3 months. The other control group was kept under the same conditions with a CE-2-based fishmeal-deprived food (CLEA). For all procedures, the animals were anesthetized with an intraperitoneal injection of 400 mg/kg Avertin (2.5% 2,2,2-tribromoethyl and tertiary amyl alcohol, v/v; Sigma-Aldrich), and the pupils were dilated with a combination of 0.5% (w/v) tropicamide and 0.5% (w/v) phenylephrine (Mydrin-P; Santen, Osaka, Japan). The use of animals in the experimental protocol was approved by the Nagoya University Animal Care Committee. All animal experiments were performed in accordance with the guidelines of the ARVO Statement for the Use of Animals in Ophthalmic and Vision Research.

Mouse model of CNV

CNV was induced by laser photocoagulation, as described previously [8, 9, 42]. To assess the laser-induced CNV (laser-CNV) volumes, 3–4 spots of laser photocoagulations (532 nm laser; power, 180 mW; duration, 100 ms; diameter, 75 μm; Novus Verdi; Coherent Inc., Santa Clara, CA, USA) were placed in the fundus of each eye on day 0 by an individual blinded to the group assignment, as described previously [43]. The laser spots were created around the optic nerve using a slit-lamp delivery system, and a coverslip was used as a contact lens. The morphologic endpoint of the laser injury was the appearance of a cavitation bubble, which is a sign of Bruch's membrane disruption. To prepare protein lysates from the tissues that were used for VEGF ELISA in the mice with intravitreal MDA injection, 16 spots of laser photocoagulations were placed in each mouse eye.

Laser-CNV volume analysis

The laser-CNV volumes were measured using a method similar to that described previously [8]. In brief, 1 week after laser injury, the eyes were enucleated and fixed with 4% (w/v) paraformaldehyde (PFA). The eyecups obtained by removing the anterior segments were incubated with 0.5% (w/v) fluorescein isothiocyanate-conjugated iB4 (Sigma-Aldrich). CNV was visualized using a blue argon laser (488 nm wavelength) and a confocal laser scanning microscope (A1-Rsi; Nikon, Tokyo, Japan). Horizontal optical sections were obtained at 1-μm intervals from the top of CNV to the surface of RPE. The images of each layer were stored digitally, and the area of CNV was measured using ImageJ software (developed by Wayne Rasband, National Institutes of Health, Bethesda, MD, USA). The summation of the whole fluorescent area in each horizontal section was used as an index for the volume of CNV. The mean volume obtained from all the laser spots (3–4 spots) per eye was calculated (*n* = number of eyes). The imaging was performed by an operator blinded to the group assignments.

Western blot analysis

After treatments, the ARPE-19 cells were washed with PBS three times and then lysed in RIPA buffer (Sigma-Aldrich) with a protease inhibitor cocktail (Roche Diagnostics). The protein lysate was conducted according to the same procedure as above. Protein (30 μg) samples from human and mouse tissues or culture cells were run on sodium dodecyl sulfate precast gels (Wako) and transferred to polyvinylidene difluoride membranes. The transferred membranes were washed in TBS-T (0.05 M Tris, 0.138 M NaCl, 0.0027 M KCl, pH = 8.0, 0.05% (v/v) Tween 20; Sigma-Aldrich) and then blocked in 5% (w/v) nonfat dry milk/TBS-T at room temperature (RT) for 2 h. The membranes were then incubated with rabbit antibody against LC3B (catalog no. 2275, 1:1000), Beclin 1 (catalog no. 3495, 1:1000; Cell Signaling Technology, Danvers, MA, USA), or p62 (catalog no. PM045, 1:1000; Medical & Biological Laboratories, Nagoya, Japan) at 4°C overnight. Protein loading was assessed by immunoblotting using anti-β-actin antibody (catalog no. 4967, 1:2000; Cell Signaling Technology). The membranes were treated with horseradish peroxidase-linked secondary antibody (catalog no. 7074, 1:3000; Cell Signaling Technology) for 1 h at RT. The signal was visualized with enhanced chemiluminescence (ECL plus; GE Healthcare, Piscataway, NJ, USA) and captured using the ImageQuant LAS-4000 imaging system (GE Healthcare).

Immunostaining

For MDA staining of human samples, eyes with wet or dry AMD and another control eye with no diagnosed ocular disease were obtained from the San Diego Eye Bank. The macular areas were cut, cryoprotected in 30% (w/v) sucrose, embedded in an optimal cutting temperature compound (Tissue-Tek OCT; Sakura Finetek, Torrance, CA, USA), and cryosectioned into 8-μm sections. Immunohistochemical staining was performed with mouse monoclonal antibody against MDA (catalog no. N213530, 1:100; NOF Corporation, Tokyo, Japan). The bound antibody was detected with a Vectastain ABC-AP kit (Vector Laboratories, Burlingame, CA, USA), and the enzyme complex was visualized with an alkaline phosphatase blue substrate kit (Vector Laboratories). Levamisole (Vector Laboratories) was used to block the endogenous alkaline phosphatase activity. The sections were then mounted, and images were taken with a BZ-9000 microscope (Keyence, Osaka, Japan). To visualize the structure of the polarized ARPE-19 cells, zonula occludens-1 (ZO-1) staining was performed in a manner similar to that described previously [4, 44]. In brief, Transwell filters were fixed with 4% PFA or 100% methanol, stained with rabbit antibodies against ZO-1 (catalog no. 617300, 1:100; Thermo Fisher Scientific, Waltham, MA, USA), and visualized with Alexa-488 (catalog no. A11008, Thermo Fisher Scientific) and Hoechst 33342 (Thermo Fisher Scientific). To examine autophagic activity, LC3 staining of cultured cells and mouse eyes was performed. For *in vitro* analysis, ARPE-19 cells were grown on chamber slides (Matsunami Glass, Tokyo, Japan); after treatment with MDA for 48 h, the cells were fixed with 100% methanol and stained with rabbit antibodies against LC3B (catalog no. 2275, 1:200; Cell Signaling Technology). For the mice fed a diet containing 15% LA, untreated eyes were enucleated and fixed with 4% PFA. Sections were prepared as described above, stained with rabbit antibodies against LC3A/B (catalog no. 12741, 1:100; Cell Signaling Technology). The LC3 staining for cultured cells and mouse eyes was visualized with Alexa-594 (catalog no. A11012, Thermo Fisher Scientific) and 4′,6-diamidino-2-phenylindole (DAPI; Thermo Fisher Scientific). Images were obtained using a confocal microscope (A1-Rsi; Nikon).

Measurement of transepithelial resistance (TER)

TER of the polarized RPE cells on the Transwell filters was measured with an Epithelial Voltohmmeter 2 (EVOM2; World Precision Instruments, Sarasota, FL, USA) as described previously [40, 41]. TER measurements were performed within 3 min after removal of

the cells from the incubator. TER (Ω) was multiplied with the effective growth area (cm^2) to obtain TER–area products ($Ω·cm^2$), the final resistance per unit area. Each well was measured at least three times, and the average value was calculated for analysis. The results are expressed as percent changes of TER relative to the control.

Mass spectrometry

After enucleating the eyes, the RPE/choroid complex was collected into double-distilled water and then frozen at −80°C. The frozen samples were dried in a freeze dryer (FD-520; EYELA, Tokyo, Japan) overnight. Measurements of fatty acids in the mouse RPE/choroid complexes and sera were performed using mass spectrometry according to modifications of previously reported methods [45, 46]. The methyl esters of LA and arachidonic acid (AA) in the sera and RPE/choroid complexes were measured using GCMS-2010Plus (Shimadzu, Kyoto, Japan) after methylation and purification using kits (Nacalai Tesque, Kyoto, Japan). A DB-5 capillary column (30 m × 0.250 mm internal diameter; 1.00 μm thickness; Agilent Technologies, Santa Clara, CA, USA) was used. The column oven temperature was held at 60°C for 1 min and then raised at 10°C/min to 320°C, which was held for 5 min. The injection port temperature and helium carrier gas flow rate were set at 280°C and 1.00 mL/min, respectively. The samples were automatically injected in the splitless mode, and the injection volume was set at 1 μL. The mass conditions were set as follows: ion source temperature, 200°C; ionization voltage, 70 eV. Relative quantitative analysis was conducted in the selected ion monitoring (SIM) mode. SIM transitions used for the analysis were as follows: *m/z* 294 and 263 for LA, 79 and 175 for AA, and 368 and 74 for tricosanoic acid as the internal standard, and the first ions with *m/z* 294, 79, and 368 were used for quantification, respectively.

Statistical analysis

The results are expressed as means ± standard errors of the mean (s.e.m.) (n = number of samples). The control sample was defined as 100%, and the percent change relative to the control was calculated for each sample. All statistical analyses were performed using version 3.2.2 of R statistical software (open-source software available at http://www.r-project.org/). Comparisons among three or more groups were analyzed with the Kruskal–Wallis test; if significance was detected ($P < 0.05$), the *post-hoc* Steel's test (for multiple-comparisons of treatment groups with the control) or Steel–Dwass test (for

all-pairs multiple comparisons) was performed. Other comparisons between two groups were analyzed statistically using the Mann–Whitney *U* test (unpaired samples). Differences were considered to be statistically significant at $P < 0.05$.

Results

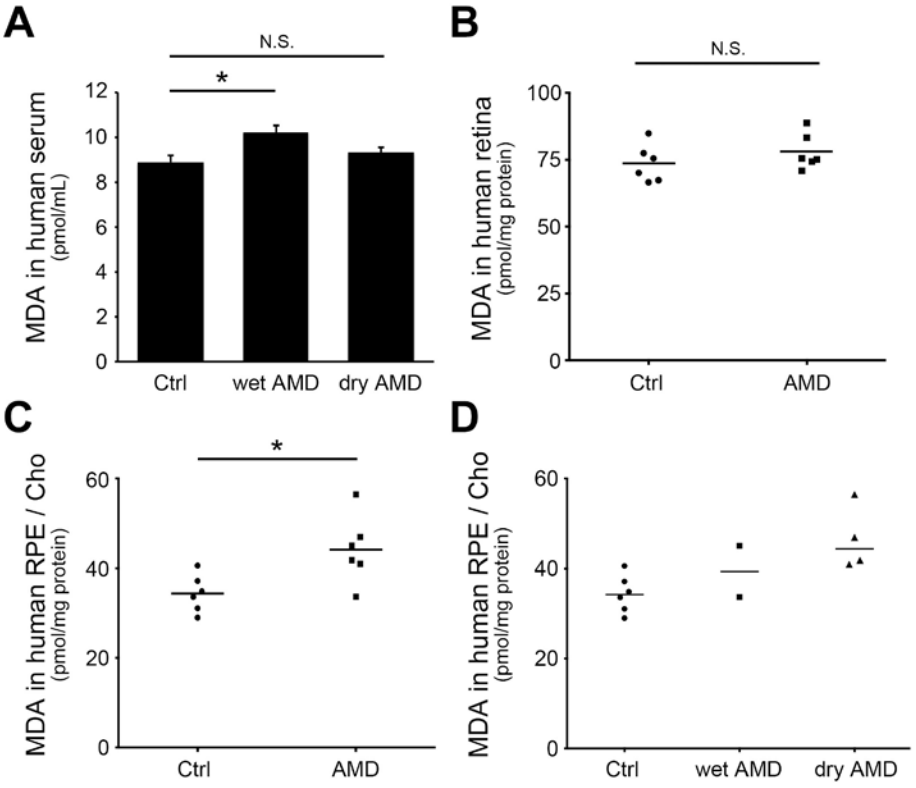

Fig. 1. MDA is increased in the sera and RPE/choroid tissues of AMD patients. (**A**) MDA levels were measured using ELISA and found to be 14.9% higher in the sera of wet AMD patients ($n = 41$ patients) than in the sera of control subjects ($n = 34$ subjects). MDA levels were also higher in the sera of dry AMD patients ($n = 19$ patients), although this was not significant. Data are expressed as the means ± s.e.m. (**B**) MDA levels were higher in the retinal tissues of AMD patients than in those of control subjects; however, the difference was not significant ($n = 6$ eyes/group). (**C**) Compared with control subject eyes, MDA levels were significantly increased by 28.5% in RPE/choroid tissues of AMD patient eyes ($n = 6$ eyes/group). (**D**) The AMD group was divided into two subgroups: wet and dry AMD. MDA levels in RPE/choroid tissues of dry AMD patients appeared to be higher than those in RPE/choroid tissues of wet AMD patients. Because of the limited sample number, statistical analysis was not performed. *: $P < 0.05$, N.S.: $P > 0.05$. Cho = choroid, Ctrl = control

MDA levels are increased in the sera and eyes of wet AMD patients

To investigate the relationship between MDA levels and AMD, we first examined MDA levels in human sera and eyes and found higher levels in the sera of AMD patients (P = 0.0169). MDA levels were 14.9% higher in the sera of wet AMD patients than in the sera of the control group (10.221 ± 0.311 pmol/mL, n = 41 patients and 8.894 ± 0.302 pmol/mL, n = 34 patients, respectively; P = 0.0114). Higher levels of MDA were also observed in the sera of dry AMD patients (9.334 ± 0.211 pmol/mL, n = 19 patients), although this was not significant (P = 0.4080; Fig. 1A). We also examined MDA levels in human eyes. Considering the limited number of samples, all AMD samples were grouped together regardless of the type of AMD. The MDA levels in the RPE/choroid of AMD patients (44.166 ± 2.817 pmol/mg protein) were increased by 28.5% (P = 0.0152, n = 6 eyes/group; Fig. 1C) compared with the levels in the control subjects (34.384 ± 1.558 pmol/mg protein). When the AMD samples were grouped according to the type of AMD (wet/dry), the MDA levels appeared to be higher in the RPE/choroid of dry AMD patients than in that of wet AMD patients (Fig. 1D; statistical analysis was not performed because of limited sample number). MDA levels in the retinal tissues of AMD patients were also measured and found to be marginally higher than those in the control subjects; however, the difference was not significant (P = 0.4156, n = 6 eyes/group; Fig. 1B). We also performed MDA staining of human eyes and found a greater degree of staining of the AMD eyes than the control eyes (Fig. 2).

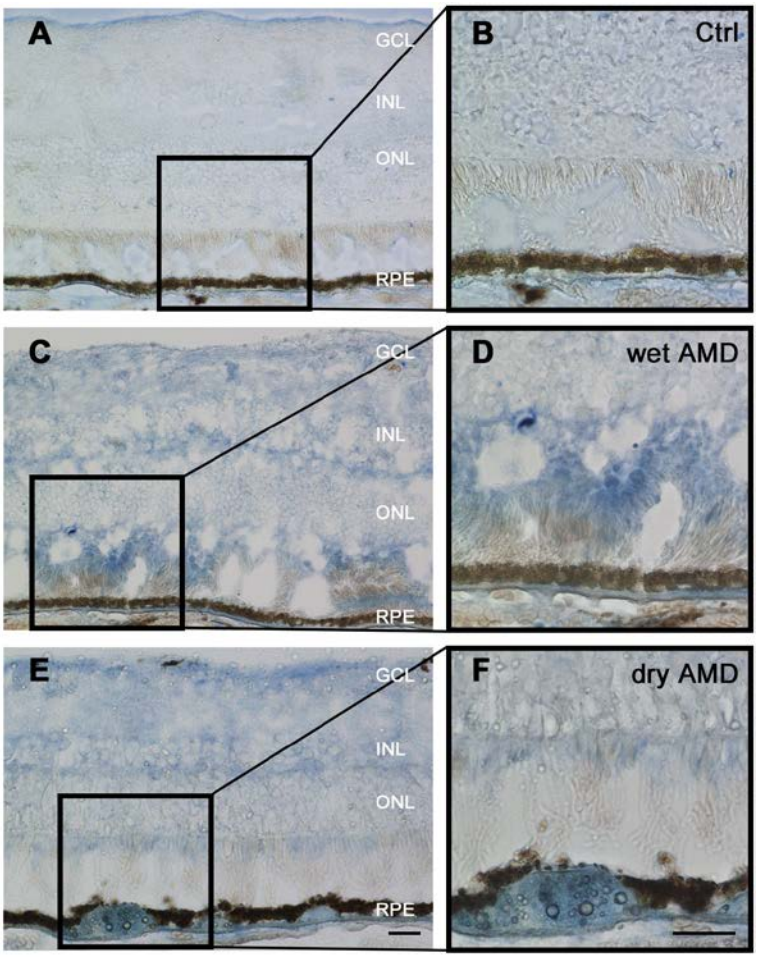

Fig. 2. AMD eyes show increased MDA staining. Eyes from control subject and patients with wet and dry AMD were sectioned and stained with MDA antibody. (**A, B**) Cryosections showing low MDA staining (blue) both in the retina and RPE in the eye with no diagnosed disease. (**C, D**) MDA staining was increased in the eye with wet AMD. (**E, F**) Cryosections from the eye with dry AMD showing increased MDA levels. (**B, D, F**) Higher resolution images showing MDA staining between the ONL and RPE layer. Scale bar = 20 μm. GCL = ganglion cell layer, INL = inner nuclear layer, ONL = outer nuclear layer, Ctrl = control

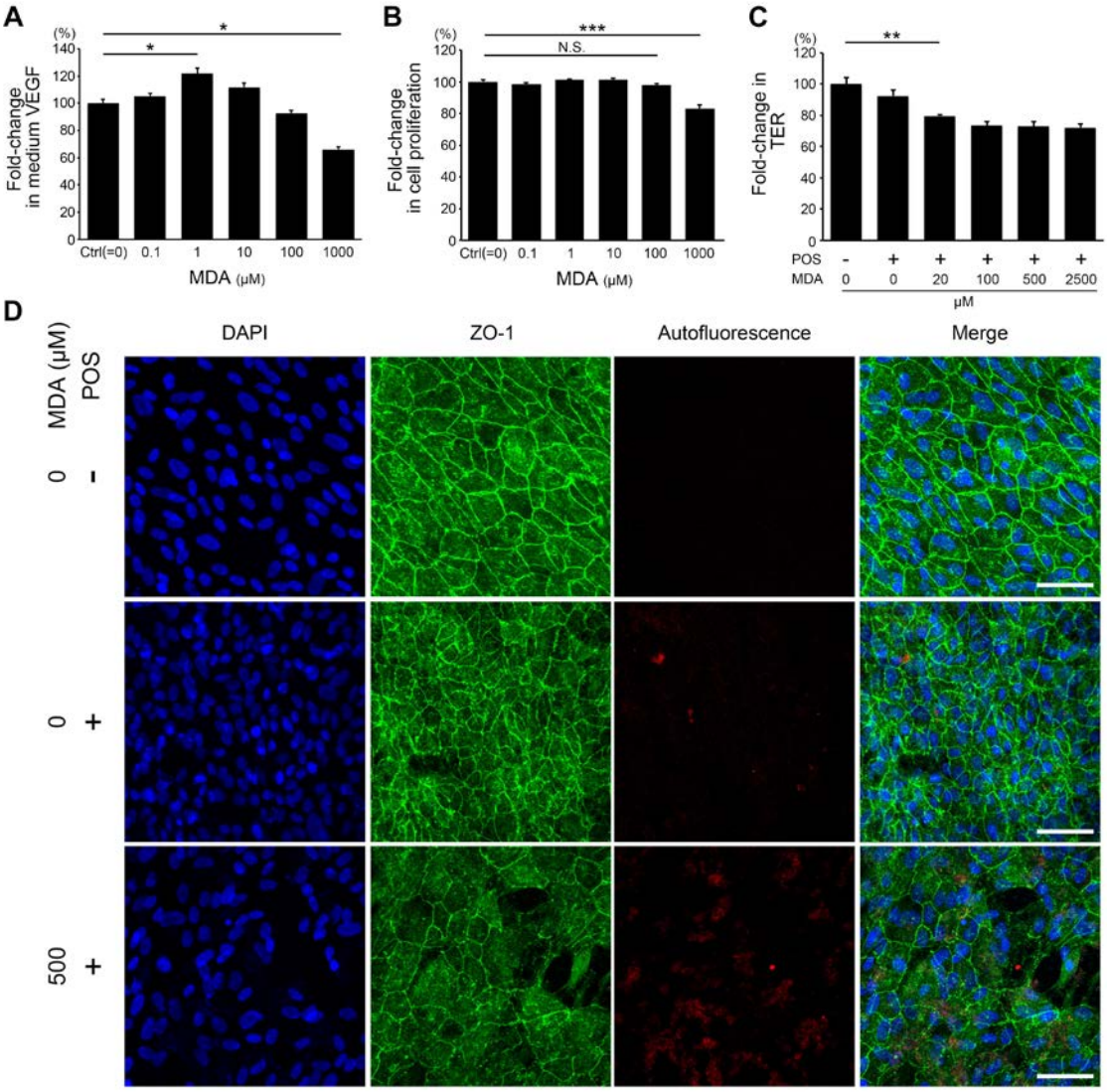

Fig. 3. Effects of MDA on ARPE-19 cells. (**A**) VEGF expression in the medium was measured using ELISA after MDA treatment for 48 h. Low-dose MDA induced VEGF expression, whereas high-dose MDA suppressed VEGF expression in ARPE-19 cells (n = 6 wells/group). (**B**) After 48 h of incubation, the proliferation ability of ARPE-19 cells was measured using the WST-1 cell proliferation assay and was found to be not significantly affected by MDA at concentrations of no more than 100 μM. Conversely, proliferation ability was significantly inhibited by 1000 μM MDA (n = 12 wells/group). (**C**) Porcine POS were modified with increasing concentrations of MDA and then washed with PBS to remove unbound MDA. Polarized ARPE-19 cells were treated with MDA-modified POS for 48 h, following which TER was measured and found to be decreased in a dose-dependent manner (n = 9 wells/group). (**D**) ZO-1 was stained in polarized ARPE-19 cells after treatment with MDA-modified POS. Autofluorescence as well as damage to structure of the RPE layer were induced by treatment of cells with MDA-modified POS. Data are expressed as the means ± s.e.m. *: $P < 0.05$, **: $P < 0.01$, ***: $P < 0.001$, N.S.: $P > 0.05$. Scale bar = 50 μm. DAPI = 4′,6-diamidino-2-phenylindole, Ctrl = control, POS = photoreceptor outer segments, TER = transepithelial resistance

MDA changes VEGF expression and disrupts cell junctions in RPE cells

Next, we examined the effects of MDA on human RPE cells *in vitro*. After treating ARPE-19 cells with MDA for 48 h, we measured the VEGF expression in the medium and found that expression was significantly changed by administration of MDA (P = 1.6710×10^{-5}, n = 6 wells/group; Fig. 3A). Interestingly, VEGF expression was increased by treatment with lower concentrations of MDA (0.1, 1, and 10 μM; P = 0.6896, 0.0174, and 0.0664, respectively) and was decreased with higher concentrations (100 and 1000 μM; P = 0.1964 and 0.0175, respectively). After 48 h of MDA treatment, the proliferation ability of the ARPE-19 cells was also examined. MDA concentrations lower than 100 μM did not induce significant differences in terms of the proliferation ability of the ARPE-19 cells (control vs. 100 μM, P = 0.5888; n = 12 wells/group). Conversely, MDA concentrations higher than 1000 μM significantly decreased the proliferation ability of the cells (control vs. 1000 μM, P = 0.0006; Fig. 3B). These results indicate that MDA has biphasic effects on VEGF expression in cultured RPE cells: a lower dose of MDA increases VEGF expression, whereas a higher dose of MDA suppresses VEGF expression, possibly because of the cytotoxicity of MDA.

In human eyes, the RPE serves functions for phagocytosing and degrading shed POS, which is vitally important for photoreceptor survival and function [25, 26]. In RPE cells, MDA adducts in POS contribute to the formation of aggregates known as lipofuscins, which are involved in the key pathological pathways of AMD [1, 3, 47]. In the present study, MDA was used to modify porcine POS for synthesizing MDA-adducted proteins. MDA-modified POS were then used to treat ARPE-19 cells with polarized culture, a monolayer cell model with conditions more closely resembling those of the human RPE sheet [39, 40]. We then measured TER, a parameter of monolayer polarized RPE cells [40]. After treating the cells with MDA-modified POS for 48 h, TER decreased in an MDA dose-dependent manner (P = 4.8270×10^{-7}, n = 9 wells/group; Fig. 3C), indicating that MDA-modified POS disrupted the junctions between the RPE cells. Following this, we stained the polarized cells with ZO-1 (an RPE junction-related molecule) [48, 49] and observed disruptions to the cell structure. An increase in lipofuscin-like autofluorescence was also observed in the polarized ARPE-19 cells after MDA-modified POS treatment (Fig. 3D).

Autophagy changes are observed in RPE of AMD patients and MDA-treated ARPE-19 cells

Next, we explored the intracellular changes in RPE caused by the presence of MDA using both human ocular samples and cell lines. Based on previous studies showing that MDA accumulates in the drusen of AMD eyes [20, 21] and that autophagic activity plays an important role in AMD pathogenesis [3, 50, 51], we hypothesized that MDA intracellularly induces changes in autophagic flux in RPE. In the present study, we used Beclin1 (a protein involved in the regulation of autophagy initiation), the ratio of LC3-II/LC3-I, and p62 (an autophagy-selective substrate, also known as SQSTM1/sequestosome 1) as indicators of autophagic activity [52, 53]. To examine changes in autophagic activities in human eyes, we performed immunoblot analysis of seven eyes with AMD and six control eyes. As shown in Fig. 4A–D, LC3B-II/LC3B-I ratio (P = 0.0023), but not Beclin 1 (P = 0.2949) were found to be significantly increased, while p62 levels were significantly decreased (P = 0.0221) in RPE of AMD patients in comparison with those in RPE of control subjects, indicating that autophagy was activated in the eyes with AMD. Consistent with our findings in human AMD eyes, MDA treatment for 48 h significantly changed the levels of autophagic activity in ARPE-19 cells *in vitro*. Low-dose MDA (0.1, 1, and 10 μM) increased the LC3B-II/LC3B-I ratio (control vs. 1 μM, P = 0.0039) and decreased the p62 levels (control vs. 1 μM, P = 0.0095) in ARPE-19 cells. Conversely, a higher dose of MDA (1000 μM) decreased the LC3B-II/LC3B-I ratio (control vs. 1000 μM, P = 0.0039) and increased the p62 levels (control vs. 1000 μM, P = 0.0095). Interestingly, we did not find any significant changes in Beclin 1 after MDA treatment (P = 0.1080). These results suggest that autophagic activity is increased by treatment with low-dose MDA but decreased by a higher dose, independently of Beclin 1 (n = 6 wells/group, Fig. 4E–G). To confirm this result, we then performed LC3 staining on ARPE-19 cells after MDA treatment, and the numbers of LC3 puncta in the cells were counted using a previously described method [53]. We found that the mean number of LC3 puncta per cell was increased by 1 μM MDA treatment (P = 0.0094) but decreased by 1000 μM MDA treatment (P = 0.0010, n = 40 cells/group; Fig. 4H,I).

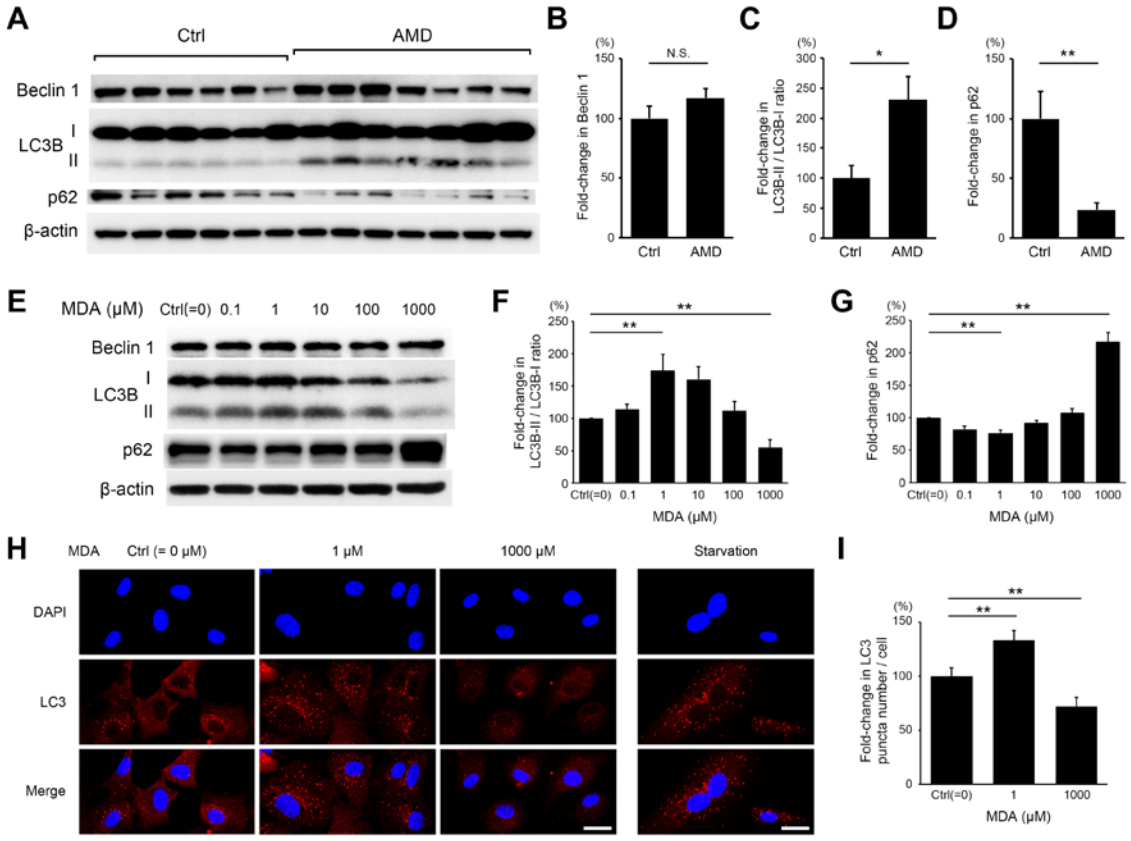

Fig. 4. Autophagy changes in RPE of AMD patients and ARPE-19 cells. (**A**) Western blot showing changes in Beclin 1, LC3B, and p62 in RPE of seven AMD eyes compared with those of six control eyes. (**B–D**) Quantitative densitometry results showing that autophagy was activated in the RPE of AMD eyes. Beclin 1 (B) was increased in AMD eyes, but with no significant difference. The ratio of LC3B-II/LC3B-I (C) was significantly increased, while p62 levels (D) were decreased. (**E**) MDA at different concentrations was used to treat ARPE-19 cells for 48 h, and western blot was performed to detect changes in Beclin 1, LC3B, and p62 levels. (**F**) Quantitative densitometry results showing that the ratio of LC3B-II/LC3B-I was increased at lower doses of MDA but decreased at higher doses (n = 6 wells/group). (**G**) Quantitative densitometry results showing the fold-changes of p62. Contrary to the results for LC3B, p62 decreased at lower doses of MDA but increased at higher doses (n = 6 wells/group). (**H**) MDA (1 and 1000 μM) was used to treat ARPE-19 cells for 48 h, and cells were stained with LC3B antibody. Representative images showing LC3 puncta in the cells that were increased by 1 μM and decreased by 1000 μM MDA. Starved cells (depletion of both L-glutamine and serum) were used as a positive control. (**I**) The mean number of LC3 puncta per cell was counted and increased by 1 μM MDA but decreased by 1000 μM MDA (n = 40 cells/group). Data are expressed as the means ± s.e.m. **: $P < 0.01$. Scale bar = 25 μm. Ctrl = control

MDA-induced VEGF increase is blocked by NH_4Cl

We also examined the relationship between VEGF secretion and autophagic activity in RPE with exposure to MDA. NH_4Cl, a lysosomal inhibitor [53], was used to block autophagic activity. Interestingly, compared with the control, the increase in VEGF caused by MDA (1 μM) was significantly blocked by NH_4Cl (20 mM) (P = 0.0206; Fig. 5A). In addition, 3-MA, an autophagy initiator inhibitor [52, 54], was also used to block autophagic activity. Similar to NH_4Cl, compared with the control, the increase in VEGF caused by MDA (1 μM) was significantly inhibited by 3-MA (10 mM) (P = 0.0095, n = 6 wells/group; Fig. 5B). However, the NH_4Cl- and 3-MA-induced blockade of autophagic activity differed. Compared with the cells treated with NH_4Cl or 3-MA alone, co-administration of MDA and NH_4Cl did not increase VEGF levels (P = 0.9951; Fig. 5A), whereas MDA still significantly increased VEGF levels in the presence of 3-MA (P = 0.0172; Fig. 5B). These results indicate that NH_4Cl does, whereas 3-MA does not, totally block the MDA-induced VEGF increase in ARPE-19 cells.

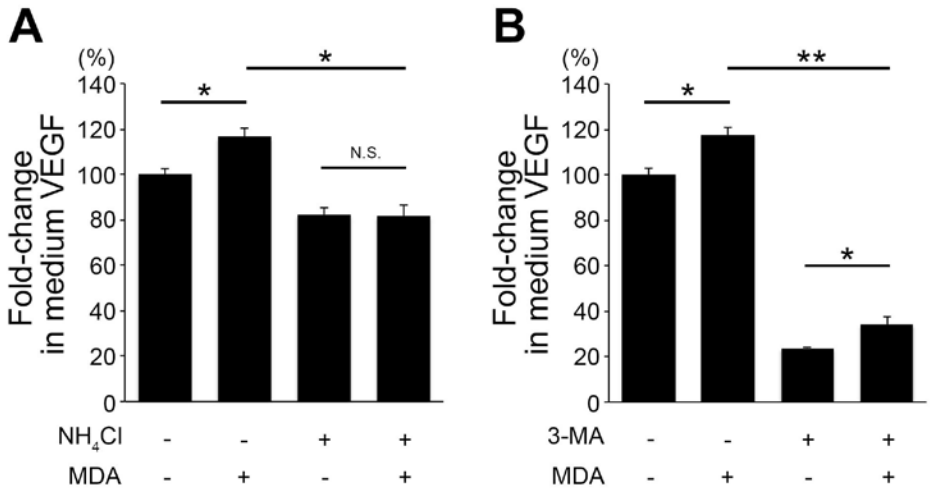

Fig. 5. NH_4Cl and 3-MA inhibit the MDA-induced VEGF increase in ARPE-19 cells. (**A**) VEGF levels were measured in the medium after treatment with 1 μM MDA and 20 mM NH_4Cl. VEGF expression was increased by 1 μM MDA; this increase was blocked by co-administration of 20 mM NH_4Cl. The co-administration of MDA and NH_4Cl did not increase VEGF levels compared with treatment with NH_4Cl alone (n = 6 wells/group). (**B**) VEGF levels were measured in the medium after treatment with 1 μM MDA and 10 mM 3-MA. VEGF expression was increased by 1 μM MDA; this increase was inhibited by the addition of 10 mM 3-MA. MDA still significantly increased VEGF levels in the presence of 3-MA (n = 6 wells/group). Data are expressed as the means ± s.e.m. *: $P < 0.05$, **: $P < 0.01$, N.S.: $P > 0.05$

Intravitreal injection of MDA increases the laser-CNV volumes

To confirm that a lower dose of MDA stimulation causes VEGF upregulation not only *in vitro* but also *in vivo*, we evaluated the laser-CNV volumes in mouse eyes with and without MDA administration. Based on previous reports regarding the volume of the vitreous cavity in mice [55-58], we injected 1 μL of 10 μM MDA in the eyes of mice (presumed final concentration of 1 μM). Compared with the injection of control PBS, intravitreal injection of MDA increased VEGF levels in the RPE/choroid tissues by 28.5% (P = 0.0030, n = 8 eyes/group; Fig. 6A) and the volumes of laser-CNV by 23.2% (P = 0.0387, n = 13 eyes/group; Fig. 6B–D).

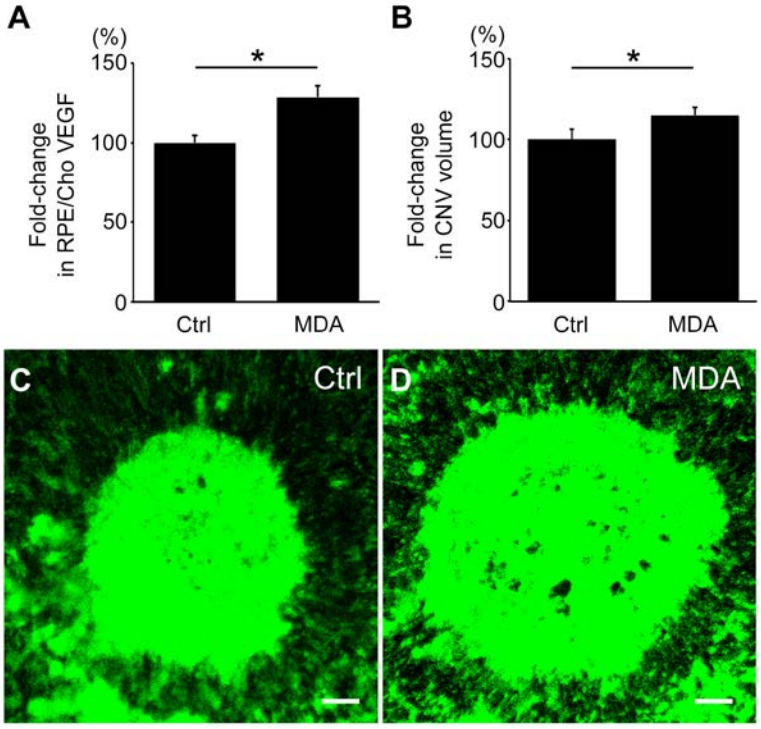

Fig. 6. Laser-CNV volumes are increased by intravitreal MDA injection. (**A**) Mice were intravitreally injected with 1 μL of 10 μM MDA (presumed final concentration of 1 μM). After laser induction, VEGF levels in the RPE/choroid tissues were measured using ELISA and found to be increased by 28.5% (n = 8 eyes/group) compared with those in mice injected with control PBS. (**B**) Compared with the control mice, the mean volume of laser-CNV was increased by 23.2% (n = 13 eyes/group) in the mice intravitreally injected with 1 μL of 10 μM MDA. (**C, D**) Representative images of laser-CNV of control mice (C) and mice injected with MDA (D). Data are expressed as the means ± s.e.m. *: $P < 0.05$. Scale bar = 50 μm. Cho = choroid, Ctrl = control

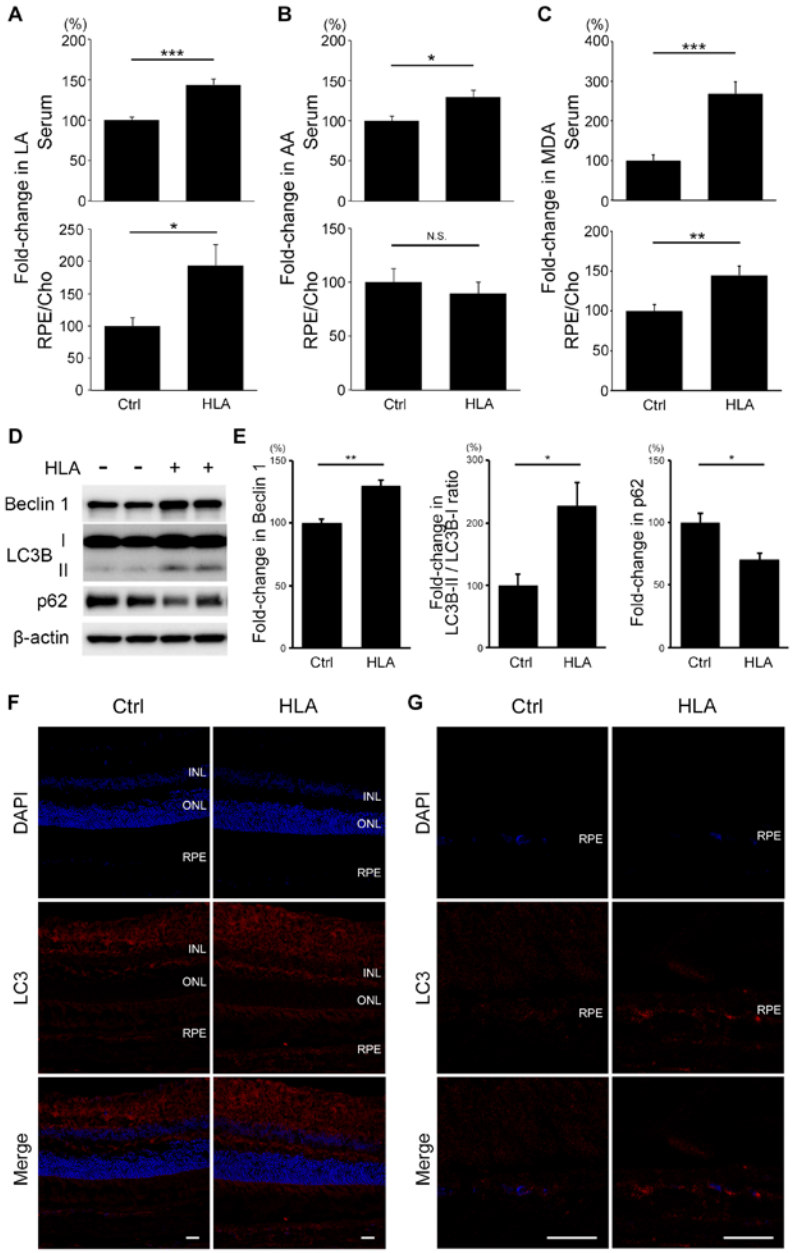

Fig. 7. LA, AA, and MDA are increased, and autophagy is activated in mice fed an HLA diet. Mice were fed an HLA diet for 3 months; LA, AA, and MDA levels were measured. (**A**) LA levels were increased in both the sera and RPE/choroid tissues (*n* = 8/group) of mice fed the HLA diet. (**B**) AA levels were increased in the sera of mice fed the HLA diet, but no significant difference was found in the RPE/choroid tissues (*n* = 8/group). (**C**) MDA levels were increased in both the sera (*n* = 20 mice/group) and RPE/choroid tissues (*n* = 8 eyes/group) of mice fed the HLA diet. (**D**) After feeding mice the HLA diet for 3 months, western blot was performed. Representative images showing changes in Beclin 1, LC3B, and p62 levels in mouse RPE/choroid tissues. (**E**) Quantitative densitometry results showing increases in Beclin 1 and the ratio of LC3B-II/LC3B-I as well as a decrease in p62 (*n* = 6 eyes/group) in the eyes of mice fed the HLA diet. (**F, G**) After feeding mice the HLA diet for 3 months, mouse eyes were stained with LC3

antibody. Representative cryosections with lower (**F**) and higher (**G**) resolutions showing more LC3 staining in the eyes of mice fed the HLA diet than in those of control mice. Data are expressed as the means ± s.e.m. *: $P < 0.05$, **: $P < 0.01$, ***: $P < 0.001$, N.S.: P > 0.05. Scale bar = 25 μm. Ctrl = control

MDA and ω-6 fatty acid levels are increased in mice fed a high-linoleic acid (HLA) diet

Clinical trials have shown that high intake of LA is a risk factor for both early onset and progression of AMD [59, 60]. Considering that MDA is an end product that is mainly generated from ω-6 fatty acid peroxidation [61], we hypothesized that LA could promote AMD development by increasing MDA. In the present study, we sought an appropriate *in vivo* model using increased dietary LA to induce abundant MDA accumulation and VEGF secretion in the eye. Therefore, we explored the effect of LA overdose in mice. Compared with mice fed the control CE-2-based fishmeal-deprived food, after being fed an HLA (15% LA) diet for 3 months, serum levels of both LA and AA were increased (LA, $P = 0.0003$; AA, $P = 0.0281$; $n = 8$ mice/group; Fig. 7A,B). In the RPE/choroid tissues, LA levels were also increased ($P = 0.0148$; Fig. 7A), whereas there was no significant change in AA levels ($P = 0.6454$, $n = 8$ eyes/group; Fig. 7B). MDA levels were also increased in both mouse sera ($n = 20$ mice/group, $P = 1.5310 \times 10^{-5}$) and RPE/choroid tissues ($n = 8$ eyes/group, $P = 0.0047$; Fig. 7C).

Autophagy is activated in mice fed an HLA diet

We also explored changes in autophagic activity. After being fed the HLA diet for 3 months, levels of Beclin 1, LC3B, and p62 in mouse RPE/choroid tissues were examined by western blotting. We found increases in Beclin 1 ($P = 0.0050$) and the ratio of LC3B-II/LC3B-I ($P = 0.0260$) as well as a decrease in p62 ($P = 0.0260$, $n = 6$ eyes/group; Fig. 7D,E). In addition, LC3 staining of cryosections showed a greater extent of LC3 staining among eyes from mice fed the HLA diet than among eyes from mice fed the control diet (Fig. 7F,G). The results above suggest that autophagy was activated in mice fed the HLA diet.

Mice fed an HLA diet show increased laser-CNV volumes

We then examined the ability of the HLA diet to increase the laser-CNV volume. Before laser induction, we enucleated mouse eyes and measured VEGF levels in RPE/choroid tissues. Compared with mice fed the control CE-2-based fishmeal-deprived diet, those fed

the HLA diet for 3 months showed increased VEGF levels (P = 0.0030, n = 8 eyes/group; Fig. 8A). After laser induction, compared with the control mice, CNV volumes were significantly increased in mice fed the HLA diet for 3 months (P = 0.0056, n = 12 eyes/group; Fig. 8B–D).

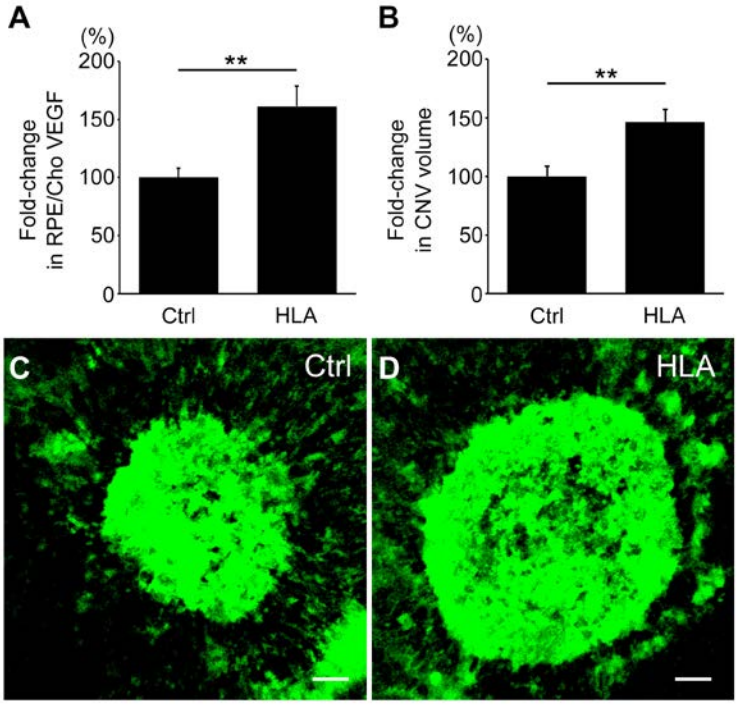

Fig. 8. Laser-CNV volumes are increased in mice fed an HLA diet. (**A**) Mice were fed an HLA diet for 3 months. VEGF levels without laser induction in RPE/choroid tissues were measured using ELISA. Compared with the control mice, VEGF levels were found to be increased by 61.4% (n = 8 eyes/group) in mice fed the HLA diet. (**B**) Laser-CNV volumes were increased by 46.5% (n = 12 eyes/group) in mice fed the HLA diet. (**C, D**) Representative images of laser-CNV of the control mice (C) and mice fed the HLA diet (D). Data are expressed as the means ± s.e.m. **: P < 0.01. Scale bar = 50 μm. Cho = choroid, Ctrl = control

Discussion

In the present study, we showed MDA accumulation in AMD eyes, which suggests that MDA might contribute to AMD pathogenesis. To our knowledge, this is the first report of quantitative measurement of MDA in human eyes. We also performed MDA staining of AMD eyes. Potassium permanganate was used in an attempt to bleach the pigment in RPE cells. However, MDA adducts were not very strong antigens as other specific proteins; they became very weak after bleaching. In the unbleached eyes with AMD, we showed increased MDA staining, which coincides with the quantitative result.

MDA reacts with proteins or nucleosides to form MDA–protein or –DNA adducts. MDA adducts are thought to be deleterious because they can induce alterations of biochemical properties and the accumulation of biomolecules in chronic diseases and during aging [61, 62]. In the present study, we showed that direct MDA treatment promotes AMD pathogenesis in both cultured RPE cells and mice. In a natural state, RPE cells are polarized and maintain a barrier function, which is important for the physiology of the retina and choroid [40, 49]. We also showed that MDA-modified POS disrupted barrier function and simultaneously induced the formation of lipofuscin-like autofluorescence. The results from using MDA-modified POS and direct MDA treatment indicate that MDA contributes to AMD pathogenesis both via the effects of preformed extracellular MDA-protein adducts and by interaction of MDA at a cellular level, potentially causing adduct formation with cellular biomolecules [61, 63]. The biphasic effects of MDA on VEGF expression in ARPE-19 cells reveal that MDA may be associated with the characterization of AMD types. Low-dose MDA induces increases in VEGF and CNV, which are observed in wet AMD eyes. Conversely, high-dose MDA causes high cytotoxicity, which induces RPE atrophy in dry AMD eyes. Moreover, in the present study, MDA levels appeared to be higher in the eyes of dry AMD patients than in those of wet AMD patients, a finding that further supports our hypothesis. Another interesting issue is that 4-hydroxynonenal, another important product of oxidative stress, has been shown to exhibit similar biphasic effects on VEGF expression in RPE cells [64, 65].

Lipid peroxidation is thought to be associated with autophagy during increased oxidative stress, and lipofuscinogenesis has also been linked to autophagy in RPE [66]. RPE is a phagocytic system that is crucial to the renewal of photoreceptors [3]. Therefore, autophagy–lysosomal dysfunction is thought to play a key role in the pathways underlying AMD pathogenesis [3, 50, 51]. We previously reported that amyloid β (Aβ), a hallmark of Alzheimer's disease, an age-related neurodegenerative disorder, was associated with induced VEGF expression in ARPE-19 cells [67]. Aβ clearance is reportedly closely related to the autophagy–lysosomal pathway [68, 69]. Meanwhile, although the effect of autophagy–lysosomal alterations on VEGF expression remains unclear [51], a previous study has reported the ability of lysosomal stress to induce VEGF expression in ARPE-19 cells [24]. In the present study, we showed autophagy dysfunction in AMD eyes. We also observed autophagy dysfunction by which MDA induces VEGF changes in cultured RPE cells. Similar to VEGF expression, the effects of

MDA on autophagy show a biphasic pattern. We speculate that MDA alters VEGF expression through the autophagy–lysosomal pathway. In the present study, we showed for the first time that an autophagy inhibitor (3-MA) and a lysosomal inhibitor (NH_4Cl) both inhibit VEGF expression in ARPE-19 cells. At the same time, the MDA-induced VEGF increase is inhibited by the autophagy and lysosomal inhibitors. The difference is that NH_4Cl totally blocks the MDA-induced increase in VEGF, whereas 3-MA only partially inhibits it. 3-MA is a phosphatidylinosital-3 kinase inhibitor, which inhibits autophagy initiation [52]. On the other hand, NH_4Cl inhibits autolysosome function [53], which is initiated after the completion of autophagy. By joint consideration of the biphasic effects of MDA on p62 clearance and LC3B-I to LC3B-II turnover independent of the levels of Beclin 1, we speculate that MDA induces autophagy dysfunction at a point between autophagy initiation and autolysosome formation. Further study is needed to identify the specific target of MDA during autophagy.

Clinical trials have shown the risk of high dietary intake of LA for AMD [59, 60]. However, little is known about how LA contributes to AMD pathogenesis *in vivo*. To our knowledge, this is the first study on AMD using dietary LA in animals. After feeding mice the HLA diet for 3 months, VEGF levels in the eyes were surprisingly elevated even before laser induction. Consequently, CNV volumes were also increased after laser induction. On the other hand, MDA levels were increased in both sera and eyes. In addition, consistent with the *in vitro* results, autophagy was activated in the eyes. This *in vivo* evidence suggests that increased MDA, which is an end product of ω-6 fatty acid peroxidation [61], played an important role in CNV progression in mice fed the HLA diet. Increased dietary LA is considered to induce relative ω-3 PUFA deficiency, which is a risk factor for many diseases, including AMD [18, 59, 70]. Our study suggests a possible pathway whereby higher dietary LA induces MDA elevation, which correspondingly induces VEGF expression and CNV formation.

Although these results revealed strong evidence for the pathogenic role and mechanism of MDA and LA in AMD, there were some limitations to this study that must be addressed. We had an insufficient number of human samples because of difficulties in acquiring donor eyes. Therefore, we were unable to statistically compare MDA levels between wet and dry AMD eyes. Moreover, further research is warranted to elucidate how and via which specific target MDA affects autophagy as well as to identify the pathway via which autophagy dysfunction alters VEGF expression.

In summary, our study showed the importance of MDA, which acts not only as a

marker but also as a causative factor of autophagy dysfunction related to AMD pathogenesis. Moreover, higher dietary intake of LA promotes CNV progression in mice with the increase in MDA levels.

Acknowledgements

The authors thank Chisato Ishizuka for her technical assistance. This work was partially supported by Grants-in-Aid for Scientific Research B (H.T.; 15H04994) and for Young Scientists A (H.K.; 25713056) from Japan Society for the Promotion of Science, Takeda Medical Research Foundation (H.K.), Takeda Science Foundation (H.K.), Japan Intractable Diseases Research Foundation (H.K.), Yokoyama Foundation for Clinical Pharmacology (YRY1411, H.K.), The Uehara Memorial Foundation (H.K.), Hori Science and Arts Foundation (F.Y.), and Mishima Saiichi Memorial Ophthalmic Research International Foundation (F.Y.).

Competing interests

No competing interests declared.

Author contributions

Fuxiang Ye: designed and performed experiments and wrote the manuscript
Hiroki Kaneko: designed and performed experiments, and wrote the manuscript
Yumi Hayashi: performed experiments
Shiang-Jyi Hwang: performed experiments
Kei Takayama: analyzed output data
Yuji Nishizawa: supervised the project
Reona Kimoto: performed experiments
Yosuke Nagasaka: analyzed output data
Taichi Tsunekawa: analyzed output data
Toshiyuki Matsuura: analyzed output data
Tsutomu Yasukawa: supervised the project
Takaaki Kondo: supervised the project
Hiroko Terasaki: supervised the project

References

[1] Ambati, J.; Ambati, B. K.; Yoo, S. H.; Ianchulev, S.; Adamis, A. P. Age-related macular degeneration: etiology, pathogenesis, and therapeutic strategies. *Surv. Ophthalmol.* **48:**257-293; 2003. doi:10.1016/S0039-6257(03)00030-4

[2] Bird, A. C. Therapeutic targets in age-related macular disease. *J. Clin. Invest.* **120:**3033-3041; 2010. doi:10.1172/JCI42437

[3] de Jong, P. T. Age-related macular degeneration. *N. Engl. J. Med.* **355:**1474-1485; 2006. doi:10.1056/NEJMra062326

[4] Kaneko, H.; Dridi, S.; Tarallo, V.; Gelfand, B. D.; Fowler, B. J.; Cho, W. G.; Kleinman, M. E.; Ponicsan, S. L.; Hauswirth, W. W.; Chiodo, V. A.; Kariko, K.; Yoo, J. W.; Lee, D. K.; Hadziahmetovic, M.; Song, Y.; Misra, S.; Chaudhuri, G.; Buaas, F. W.; Braun, R. E.; Hinton, D. R.; Zhang, Q.; Grossniklaus, H. E.; Provis, J. M.; Madigan, M. C.; Milam, A. H.; Justice, N. L.; Albuquerque, R. J.; Blandford, A. D.; Bogdanovich, S.; Hirano, Y.; Witta, J.; Fuchs, E.; Littman, D. R.; Ambati, B. K.; Rudin, C. M.; Chong, M. M.; Provost, P.; Kugel, J. F.; Goodrich, J. A.; Dunaief, J. L.; Baffi, J. Z.; Ambati, J. DICER1 deficit induces Alu RNA toxicity in age-related macular degeneration. *Nature* **471:**325-330; 2011. doi:10.1038/nature09830

[5] Brown, D. M.; Kaiser, P. K.; Michels, M.; Soubrane, G.; Heier, J. S.; Kim, R. Y.; Sy, J. P.; Schneider, S.; Group, A. S. Ranibizumab versus verteporfin for neovascular age-related macular degeneration. *N. Engl. J. Med.* **355:**1432-1444; 2006. doi:10.1056/NEJMoa062655

[6] Gragoudas, E. S.; Adamis, A. P.; Cunningham, E. T., Jr.; Feinsod, M.; Guyer, D. R.; Group, V. I. S. i. O. N. C. T. Pegaptanib for neovascular age-related macular degeneration. *N. Engl. J. Med.* **351:**2805-2816; 2004. doi:10.1056/NEJMoa042760

[7] Rosenfeld, P. J.; Brown, D. M.; Heier, J. S.; Boyer, D. S.; Kaiser, P. K.; Chung, C. Y.; Kim, R. Y.; Group, M. S. Ranibizumab for neovascular age-related macular degeneration. *N. Engl. J. Med.* **355:**1419-1431; 2006. doi:10.1056/NEJMoa054481

[8] Ye, F.; Kaneko, H.; Nagasaka, Y.; Ijima, R.; Nakamura, K.; Nagaya, M.; Takayama, K.; Kajiyama, H.; Senga, T.; Tanaka, H.; Mizuno, M.; Kikkawa, F.; Hori, M.; Terasaki, H. Plasma-activated medium suppresses choroidal neovascularization in mice: a new therapeutic concept for age-related macular degeneration. *Sci. Rep.* **5:**7705; 2015. doi:10.1038/srep07705

[9] Kaneko, H.; Ye, F.; Ijima, R.; Kachi, S.; Kato, S.; Nagaya, M.; Higuchi, A.; Terasaki, H. Histamine H4 receptor as a new therapeutic target for choroidal neovascularization in age-related macular degeneration. *Br. J. Pharmacol.* **171:**3754-3763; 2014. doi:10.1111/bph.12737

[10] Rofagha, S.; Bhisitkul, R. B.; Boyer, D. S.; Sadda, S. R.; Zhang, K.; Group, S.-U. S. Seven-year outcomes in ranibizumab-treated patients in ANCHOR, MARINA, and HORIZON: a multicenter cohort study (SEVEN-UP). *Ophthalmology* **120:**2292-2299; 2013. doi:10.1016/j.ophtha.2013.03.046

[11] Clemons, T. E.; Milton, R. C.; Klein, R.; Seddon, J. M.; Ferris, F. L., 3rd; Age-Related Eye Disease Study Research, G. Risk factors for the incidence of Advanced Age-Related Macular Degeneration in the Age-Related Eye Disease Study (AREDS) AREDS report no. 19. *Ophthalmology* **112:**533-539; 2005. doi:10.1016/j.ophtha.2004.10.047

[12] Klein, R.; Peto, T.; Bird, A.; Vannewkirk, M. R. The epidemiology of age-related macular degeneration. *Am. J. Ophthalmol.* **137:**486-495; 2004. doi:10.1016/j.ajo.2003.11.069

[13] Vingerling, J. R.; Dielemans, I.; Bots, M. L.; Hofman, A.; Grobbee, D. E.; de Jong, P. T. Age-related macular degeneration is associated with atherosclerosis. The Rotterdam Study. *Am. J. Epidemiol.* **142:**404-409; 1995.

[14] Beatty, S.; Koh, H.; Phil, M.; Henson, D.; Boulton, M. The role of oxidative stress in the pathogenesis of age-related macular degeneration. *Surv. Ophthalmol.* **45:**115-134; 2000. doi:10.1016/S0039-6257(00)00140-5

[15] Esterbauer, H.; Schaur, R. J.; Zollner, H. Chemistry and biochemistry of 4-hydroxynonenal, malonaldehyde and related aldehydes. *Free Radic. Biol. Med.* **11:**81-128; 1991. doi:10.1016/0891-5849(91)90192- 6

[16] Njie-Mbye, Y. F.; Kulkarni-Chitnis, M.; Opere, C. A.; Barrett, A.; Ohia, S. E. Lipid peroxidation: pathophysiological and pharmacological implications in the eye. *Front. Physiol.* **4:**366; 2013. doi:10.3389/fphys.2013.00366

[17] Farvid, M. S.; Ding, M.; Pan, A.; Sun, Q.; Chiuve, S. E.; Steffen, L. M.; Willett, W. C.; Hu, F. B. Dietary linoleic acid and risk of coronary heart disease: a systematic review and meta-analysis of prospective cohort studies. *Circulation* **130:**1568-1578; 2014. doi:10.1161/CIRCULATIONAHA.114.010236

[18] Okuyama, H.; Kobayashi, T.; Watanabe, S. Dietary fatty acids--the N-6/N-3 balance and chronic elderly diseases. Excess linoleic acid and relative N-3 deficiency syndrome seen in Japan. *Prog. Lipid Res.* **35:**409-457; 1996. doi:10.1016/S0163-7827(96) 00012- 4

[19] Ramsden, C. E.; Zamora, D.; Leelarthaepin, B.; Majchrzak-Hong, S. F.; Faurot, K. R.; Suchindran, C. M.; Ringel, A.; Davis, J. M.; Hibbeln, J. R. Use of dietary linoleic acid for secondary prevention of coronary heart disease and death: evaluation of recovered data from the Sydney Diet Heart Study and updated meta-analysis. *BMJ* **346:**e8707; 2013. doi:10.1136/bmj.e8707

[20] Schutt, F.; Bergmann, M.; Holz, F. G.; Kopitz, J. Proteins modified by malondialdehyde, 4-hydroxynonenal, or advanced glycation end products in lipofuscin of human retinal pigment epithelium. *Invest. Ophthalmol. Vis. Sci.* **44:**3663-3668; 2003. doi:10.1167/iovs.03-0172

[21] Weismann, D.; Hartvigsen, K.; Lauer, N.; Bennett, K. L.; Scholl, H. P.; Charbel Issa, P.; Cano, M.; Brandstatter, H.; Tsimikas, S.; Skerka, C.; Superti-Furga, G.; Handa, J. T.; Zipfel, P. F.; Witztum, J. L.; Binder, C. J. Complement factor H binds malondialdehyde epitopes and protects from oxidative stress. *Nature* **478:**76-81; 2011. doi:10.1038/nature10449

[22] Del Rio, D.; Stewart, A. J.; Pellegrini, N. A review of recent studies on malondialdehyde as toxic molecule and biological marker of oxidative stress. *Nutr. Metab. Cardiovasc. Dis.* **15:**316-328; 2005. doi:10.1016/j.numecd.2005.05.003

[23] Niedernhofer, L. J.; Daniels, J. S.; Rouzer, C. A.; Greene, R. E.; Marnett, L. J. Malondialdehyde, a product of lipid peroxidation, is mutagenic in human cells. *J. Biol. Chem.* **278:**31426-31433; 2003. doi:10.1074/jbc.M212549200

[24] Bergmann, M.; Holz, F.; Kopitz, J. Lysosomal stress and lipid peroxidation products induce VEGF-121 and VEGF-165 expression in ARPE-19 cells. *Graefes Arch. Clin. Exp. Ophthalmol.* **249:**1477-1483; 2011. doi:10.1007/s00417-011-1682-0

[25] Krohne, T. U.; Stratmann, N. K.; Kopitz, J.; Holz, F. G. Effects of lipid peroxidation products on lipofuscinogenesis and autophagy in human retinal pigment epithelial cells. *Exp. Eye Res.* **90:**465-471; 2010. doi:10.1016/j.exer.2009.12.011

[26] Krohne, T. U.; Kaemmerer, E.; Holz, F. G.; Kopitz, J. Lipid peroxidation products reduce lysosomal protease activities in human retinal pigment epithelial cells via two different mechanisms of action. *Exp. Eye Res.* **90:**261-266; 2010. doi:10.1016/j.exer.2009.10.014

[27] Shen, X. L.; Jia, J. H.; Zhao, P.; Fan, R.; Pan, X. Y.; Yang, H. M.; Liu, L. Changes in blood oxidative and antioxidant parameters in a group of Chinese patients with age-related macular degeneration. *J. Nutr. Health Aging* **16:**201-204; 2012. doi:10.1007/s12603- 011- 0350- 8

[28] Totan, Y.; Cekic, O.; Borazan, M.; Uz, E.; Sogut, S.; Akyol, O. Plasma malondialdehyde and nitric oxide levels in age related macular degeneration. *Br. J. Ophthalmol.* **85:**1426-1428; 2001. doi:10.1136/bjo.85.12.1426

[29] Yildirim, O.; Ates, N. A.; Tamer, L.; Muslu, N.; Ercan, B.; Atik, U.; Kanik, A. Changes in antioxidant enzyme activity and malondialdehyde level in patients with age-related macular degeneration. *Ophthalmologica* **218:**202-206; 2004. doi:10.1159/000076845

[30] Brzek, P.; Ksiazek, A.; Oldakowski, L.; Konarzewski, M. High basal metabolic rate does not elevate oxidative stress during reproduction in laboratory mice. *J. Exp. Biol.* **217:**1504-1509; 2014. doi:10.1242/jeb.100073

[31] ElAli, A.; Doeppner, T. R.; Zechariah, A.; Hermann, D. M. Increased blood-brain barrier permeability and brain edema after focal cerebral ischemia induced by hyperlipidemia: role of lipid peroxidation and calpain-1/2, matrix metalloproteinase-2/9, and RhoA overactivation. *Stroke* **42:**3238-3244; 2011. doi:10.1161/STROKEAHA.111.615559

[32] Muhlfeld, C.; Das, S. K.; Heinzel, F. R.; Schmidt, A.; Post, H.; Schauer, S.; Papadakis, T.; Kummer, W.; Hoefler, G. Cancer induces cardiomyocyte remodeling and hypoinnervation in the left ventricle of the mouse heart. *PLoS One* **6:**e20424; 2011. doi:10.1371/journal.pone.0020424

[33] Imai, H.; Arai, Z. Hydrolysis of 1,1,3,3-tetramethoxypropane and spectrophotometric determination of its product, malondialdehyde. *Bunseki kagaku* **40:**143-147; 1991. doi:10.2116/bunsekikagaku.40.3_143

[34] Kwon, T. W.; Watts, B. M. Determination of Malonaldehyde by Ultraviolet Spectrophotometry. *J. Food Sci.* **28:**627-630; 1963. doi:Doi 10.1111/J.1365-2621.1963.Tb01666.X

[35] Lung, C. C.; Fleisher, J. H.; Meinke, G.; Pinnas, J. L. Immunochemical properties of malondialdehyde-protein adducts. *J. Immunol. Methods* **128:**127-132; 1990. doi:10.1016/ 0022-1759(90)90471-7

[36] Schraermeyer, U.; Enzmann, V.; Kohen, L.; Addicks, K.; Wiedemann, P.; Heimann, K. Porcine iris pigment epithelial cells can take up retinal outer segments. *Exp. Eye Res.* **65:**277-287; 1997. doi:10.1006/exer.1997.0339

[37] Kaemmerer, E.; Schutt, F.; Krohne, T. U.; Holz, F. G.; Kopitz, J. Effects of lipid peroxidation-related protein modifications on RPE lysosomal functions and POS phagocytosis. *Invest. Ophthalmol. Vis. Sci.* **48:**1342-1347; 2007. doi:10.1167/iovs.06-0549

[38] Dunn, K. C.; Aotaki-Keen, A. E.; Putkey, F. R.; Hjelmeland, L. M. ARPE-19, a human retinal pigment epithelial cell line with differentiated properties. *Exp. Eye Res.* **62:**155-169; 1996. doi:10.1006/exer.1996.0020

[39] Maminishkis, A.; Chen, S.; Jalickee, S.; Banzon, T.; Shi, G.; Wang, F. E.; Ehalt, T.; Hammer, J. A.; Miller, S. S. Confluent monolayers of cultured human fetal retinal pigment epithelium exhibit morphology and physiology of native tissue. *Invest. Ophthalmol. Vis. Sci.* **47:**3612-3624; 2006. doi:10.1167/iovs.05-1622

[40] Sonoda, S.; Spee, C.; Barron, E.; Ryan, S. J.; Kannan, R.; Hinton, D. R. A protocol for the culture and differentiation of highly polarized human retinal pigment epithelial cells. *Nat. Protoc.* **4:**662-673; 2009. doi:10.1038/nprot.2009.33

[41] Terasaki, H.; Shirasawa, M.; Otsuka, H.; Yamashita, T.; Uchino, E.; Hisatomi, T.; Sonoda, S.; Sakamoto, T. Different Effects of Thrombin on VEGF Secretion, Proliferation, and Permeability in Polarized and Non-polarized Retinal Pigment Epithelial Cells. *Curr. Eye Res.* **40:**936-945; 2015. doi:10.3109/02713683.2014.964417

[42] Ijima, R.; Kaneko, H.; Ye, F.; Takayama, K.; Nagasaka, Y.; Kataoka, K.; Funahashi, Y.; Iwase, T.; Kachi, S.; Kato, S.; Terasaki, H. Suppression of Laser-Induced Choroidal Neovascularization by the Oral Medicine Targeting Histamine Receptor H4 in Mice. *Transl Vis Sci Technol* **4:**6; 2015. doi:10.1167/tvst.4.2.6

[43] Tomida, D.; Nishiguchi, K. M.; Kataoka, K.; Yasuma, T. R.; Iwata, E.; Uetani, R.; Kachi, S.; Terasaki, H. Suppression of choroidal neovascularization and quantitative and qualitative inhibition of VEGF and CCL2 by heparin. *Invest. Ophthalmol. Vis. Sci.* **52:**3193-3199; 2011. doi:10.1167/iovs.10-6737

[44] Ijima, R.; Kaneko, H.; Ye, F.; Nagasaka, Y.; Takayama, K.; Kataoka, K.; Kachi, S.; Iwase, T.; Terasaki, H. Interleukin-18 induces retinal pigment epithelium degeneration in mice. *Invest. Ophthalmol. Vis. Sci.* **55:**6673-6678; 2014. doi:10.1167/iovs.14-15367

[45] Kawano, Y.; Nishiumi, S.; Tanaka, S.; Nobutani, K.; Miki, A.; Yano, Y.; Seo, Y.; Kutsumi, H.; Ashida, H.; Azuma, T.; Yoshida, M. Activation of the aryl hydrocarbon receptor induces hepatic steatosis via the upregulation of fatty acid transport. *Arch. Biochem. Biophys.* **504:**221-227; 2010. doi:10.1016/j.abb.2010.09.001

[46] Zaitsu, K.; Hayashi, Y.; Suzuki, K.; Nakayama, H.; Hattori, N.; Takahara, R.; Kusano, M.; Tsuchihashi, H.; Ishii, A. Metabolome disruption of the rat cerebrum induced by the acute toxic effects of the synthetic cannabinoid MAM-2201. *Life Sci.* **137:**49-55; 2015. doi:10.1016/j.lfs.2015.05.013

[47] Saadat, K. A.; Murakami, Y.; Tan, X.; Nomura, Y.; Yasukawa, T.; Okada, E.; Ikeda, Y.; Yanagi, Y. Inhibition of autophagy induces retinal pigment epithelial cell damage by the lipofuscin fluorophore A2E. *FEBS Open Bio* **4:**1007-1014; 2014. doi:10.1016/j.fob.2014.11.003

[48] Liang, C. M.; Tai, M. C.; Chang, Y. H.; Chen, Y. H.; Chen, C. L.; Lu, D. W.; Chen, J. T. Glucosamine inhibits epithelial-to-mesenchymal transition and migration of retinal pigment epithelium cells in culture and morphologic changes in a mouse model of proliferative vitreoretinopathy. *Acta Ophthalmol* **89:**e505-514; 2011. doi:10.1111/j.1755-3768.2011.02147.x

[49] Shirasawa, M.; Sonoda, S.; Terasaki, H.; Arimura, N.; Otsuka, H.; Yamashita, T.; Uchino, E.; Hisatomi, T.; Ishibashi, T.; Sakamoto, T. TNF-alpha disrupts morphologic and functional barrier properties of polarized retinal pigment epithelium. *Exp. Eye Res.* **110:**59-69; 2013. doi:10.1016/j.exer.2013.02.012

[50] Kaarniranta, K.; Sinha, D.; Blasiak, J.; Kauppinen, A.; Vereb, Z.; Salminen, A.; Boulton, M. E.; Petrovski, G. Autophagy and heterophagy dysregulation leads to retinal pigment epithelium dysfunction and development of age-related macular degeneration. *Autophagy* **9:**973-984; 2013. doi:10.4161/auto.24546

[51] Klettner, A.; Kauppinen, A.; Blasiak, J.; Roider, J.; Salminen, A.; Kaarniranta, K. Cellular and molecular mechanisms of age-related macular degeneration: from impaired autophagy to neovascularization. *Int. J. Biochem. Cell Biol.* **45:**1457-1467; 2013. doi:10.1016/j.biocel.2013.04.013

[52] Ding, W. X.; Manley, S.; Ni, H. M. The emerging role of autophagy in alcoholic liver disease. *Exp. Biol. Med. (Maywood)* **236:**546-556; 2011. doi:10.1258/ebm.2011.010360

[53] Mizushima, N.; Yoshimori, T.; Levine, B. Methods in mammalian autophagy research. *Cell* **140:**313-326; 2010. doi:10.1016/j.cell.2010.01.028

[54] Rubinsztein, D. C.; Codogno, P.; Levine, B. Autophagy modulation as a potential therapeutic target for diverse diseases. *Nat. Rev. Drug Discov.* **11:**709-730; 2012. doi:10.1038/nrd3802

[55] Lebrun-Julien, F.; Bertrand, M. J.; De Backer, O.; Stellwagen, D.; Morales, C. R.; Di Polo, A.; Barker, P. A. ProNGF induces TNFalpha-dependent death of retinal ganglion cells through a p75NTR non-cell-autonomous signaling pathway. *Proc. Natl. Acad. Sci. USA* **107:**3817-3822; 2010. doi:10.1073/pnas.0909276107

[56] Remtulla, S.; Hallett, P. E. A schematic eye for the mouse, and comparisons with the rat. *Vision Res.* **25:**21-31; 1985.

[57] Yu, D. Y.; Cringle, S. J. Oxygen distribution in the mouse retina. *Invest. Ophthalmol. Vis. Sci.*

47:1109-1112; 2006. doi:10.1167/iovs.05-1118
[58] Sharma, S.; Ball, S. L.; Peachey, N. S. Pharmacological studies of the mouse cone electroretinogram. *Vis. Neurosci.* **22:**631-636; 2005. doi:10.1017/S0952523805225129
[59] Tan, J. S.; Wang, J. J.; Flood, V.; Mitchell, P. Dietary fatty acids and the 10-year incidence of age-related macular degeneration: the Blue Mountains Eye Study. *Arch. Ophthalmol.* **127:**656-665; 2009. doi:10.1001/archophthalmol.2009.76
[60] Seddon, J. M.; Cote, J.; Rosner, B. Progression of age-related macular degeneration: association with dietary fat, transunsaturated fat, nuts, and fish intake. *Arch. Ophthalmol.* **121:**1728-1737; 2003. doi:10.1001/archopht.121.12.1728
[61] Ayala, A.; Munoz, M. F.; Arguelles, S. Lipid peroxidation: production, metabolism, and signaling mechanisms of malondialdehyde and 4-hydroxy-2-nonenal. *Oxid. Med. Cell. Longev.* **2014:**360438; 2014. doi:10.1155/2014/360438
[62] Hohn, A.; Konig, J.; Grune, T. Protein oxidation in aging and the removal of oxidized proteins. *J. Proteomics* **92:**132-159; 2013. doi:10.1016/j.jprot.2013.01.004
[63] Pizzimenti, S.; Ciamporcero, E.; Daga, M.; Pettazzoni, P.; Arcaro, A.; Cetrangolo, G.; Minelli, R.; Dianzani, C.; Lepore, A.; Gentile, F.; Barrera, G. Interaction of aldehydes derived from lipid peroxidation and membrane proteins. *Front. Physiol.* **4:**242; 2013. doi:10.3389/fphys.2013.00242
[64] Ayalasomayajula, S. P.; Kompella, U. B. Induction of vascular endothelial growth factor by 4-hydroxynonenal and its prevention by glutathione precursors in retinal pigment epithelial cells. *Eur. J. Pharmacol.* **449:**213-220; 2002. doi:10.1016/S0014-2999(02)02043-5
[65] Vatsyayan, R.; Lelsani, P. C.; Chaudhary, P.; Kumar, S.; Awasthi, S.; Awasthi, Y. C. The expression and function of vascular endothelial growth factor in retinal pigment epithelial (RPE) cells is regulated by 4-hydroxynonenal (HNE) and glutathione S-transferaseA4-4. *Biochem. Biophys. Res. Commun.* **417:**346-351; 2012. doi:10.1016/j.bbrc.2011.11.113
[66] Dodson, M.; Darley-Usmar, V.; Zhang, J. Cellular metabolic and autophagic pathways: traffic control by redox signaling. *Free Radic. Biol. Med.* **63:**207-221; 2013. doi:10.1016/j.freeradbiomed.2013.05.014
[67] Matsui, A.; Kaneko, H.; Kachi, S.; Ye, F.; Hwang, S. J.; Takayama, K.; Nagasaka, Y.; Sugita, T.; Terasaki, H. Expression of Vascular Endothelial Growth Factor by Retinal Pigment Epithelial Cells Induced by Amyloid-beta Is Depressed by an Endoplasmic Reticulum Stress Inhibitor. *Ophthalmic Res.* **55:**37-44; 2015. doi:10.1159/000440885
[68] Zhao, H.; Wang, Z. C.; Wang, K. F.; Chen, X. Y. Abeta peptide secretion is reduced by Radix Polygalaeinduced autophagy via activation of the AMPK/mTOR pathway. *Mol. Med. Rep.* **12:**2771-2776; 2015. doi:10.3892/mmr.2015.3781
[69] Cai, Z.; Chen, G.; He, W.; Xiao, M.; Yan, L. J. Activation of mTOR: a culprit of Alzheimer's disease? *Neuropsychiatr. Dis. Treat.* **11:**1015-1030; 2015. doi:10.2147/NDT.S75717
[70] Gibson, R. A.; Muhlhausler, B.; Makrides, M. Conversion of linoleic acid and alpha-linolenic acid to long-chain polyunsaturated fatty acids (LCPUFAs), with a focus on pregnancy, lactation and the first 2 years of life. *Matern. Child Nutr.* **7 Suppl 2:**17-26; 2011. doi:10.1111/j.1740-8709.2011.00299.x